

# Constant Force Actuator for Gravitational Wave Detector's

## Seismic Attenuation Systems (SAS)

Chenyang Wang<sup>a(\*)</sup>, Hareem Tariq<sup>a,b</sup>, Riccardo DeSalvo<sup>a(\*)</sup>, Yuki Yoshi Iida<sup>c</sup>, Szabolcs Marka<sup>a</sup>,

Yuhiko Nishi<sup>c</sup>, Virginio Sannibale<sup>a</sup>, Akiteru Takamori<sup>c</sup>

a) LIGO project, California Institute of Technology, 1200 E. California Bl., Pasadena, CA, 91125, USA

b) Florida Institute of Technology, 150 W. University Bl., Melbourne, FL, 32901, USA

c) Department of Physics, University of Tokyo, 7-3-1 Hongo, Bunkyo-ku, Tokyo 113-0033, Japan

(\*) corresponding authors, [chenyang@its.caltech.edu](mailto:chenyang@its.caltech.edu), [desalvo@ligo.caltech.edu](mailto:desalvo@ligo.caltech.edu)

### Abstract

We have designed, tested and implemented a UHV-compatible, low-noise, non-contacting force actuator for DC positioning and inertial damping of the rigid body resonances of the Seismic Attenuation System designed for the TAMA Gravitational Wave Interferometer. The actuator fully satisfies the stringent zero-force-gradient requirements that are necessary to prevent re-injecting seismic noise into the SAS chain. The actuator's closed magnetic field design makes for particularly low power requirements, and low susceptibility to external perturbations. The actuator retains enough strength to absorb seismic perturbations even during small earthquakes.

PACS: 04.80.Nn, 95.30.Sf, 95.55Ym.

Keywords: Gravitational Wave Interferometers, Seismic Isolation, Inertial Mode Damping

Constant Force Actuators

Proof address: Riccardo DeSalvo, LIGO Project, Mail Station 18-34, California Institute of Technology,  
1200 E. California Bl., Pasadena, CA 91125, USA

Tel ++ 1 626 395 2968

Fax ++ 1 626 395 3814

e-mail [desalvo@ligo.caltech.edu](mailto:desalvo@ligo.caltech.edu)

## 1. INTRODUCTION

Interferometric Gravitational Wave (GW) Detectors must be isolated from the seismic motion disturbances in order to be sensitive to the GW signals whose predicted amplitude is less than  $10^{-18}$  m/Hz<sup>1/2</sup> @ 10 Hz. The required isolation is obtained by means of a passive mechanical Seismic Attenuation System (SAS) [1-5] which is made of an Inverted Pendulum<sup>[6]</sup> (IP), followed by a chain of passive mechanical oscillators (filters). [7-12] The IP and the filter chain adequately isolate each interferometer mirror above 4 to 6 Hz by means of mechanical resonances carefully positioned between a few tens of mHz and 3 to 4 Hz. These resonances excited by seismic motion can reach large excursions, thus causing the mirror payload to move by several microns at low frequency. This residual motion requires large mirror control authority<sup>A</sup> to maintain phase lock in the resonant cavities of the interferometer.<sup>[13]</sup> Since the noise of an amplifier is typically a fraction of its maximum output, large authority on the mirror translates into large actuation noise. To suppress the unwanted residual motion (and eliminate the mirror actuation noise), we use an active resonance damping system whose correction signal is generated by Linear Variable Differential Transformer (LVDT)<sup>[14]</sup> position sensors and horizontal accelerometers<sup>[15]</sup>. These instruments detect the movement of the IP as it recoils from the low frequency chain oscillations, and generate feedback signals for damping actuators. The LVDT sensors are also used for positioning the mirror suspension point. See Reference [2] and Reference [16] for a description of typical control loops.

The object of the damping actuator's design is to provide the forces necessary for both damping and positioning.

A force provided by the actuators would re-introduce seismic noise when the exerted force is dependent on the relative movements of the IP table. If the actuator force has any dependence on position, seismic vibrations applied to the actuator support will partially re-inject seismic noise onto the IP table. For the same reason, the actuator must also be non-contacting. Any part of the actuator making contact between its support and the IP table will, to some degree, short circuit seismic noise onto it.

---

<sup>A</sup> The mirror must be controlled to  $\ll 10^{-12}$  precision and  $\ll 10^{-18}$  noise above 5Hz. This is achieved through a three-step system of hierarchical control authority allocation. The actuation on the mirror itself is allowed to work at comparatively high frequency (<10 Hz) but extremely small dynamic ranges ( $< 10^{-14}m$ ), while the upper stages control the mirror suspension point at progressively lower frequency and wider dynamic range.

It is necessary to design a linear contact-free actuator that produces a force independent of its position in all three directions in space. The good IP passive attenuation performance and its large positioning dynamic range require that the constant force actuator operate over at least 10 mm in the horizontal plane, and 1 mm in the vertical direction, with less than 1% force variation over the full range.

In the Virgo seismic isolation system the contact-free actuator was achieved using two large coils in a Maxwell pair configuration, and a small permanent dipole magnet in the central volume of constant field gradient <sup>[17]</sup>. In the Maxwell pair, the two coils are positioned so that the increasing field gradient of one coil is canceled by a corresponding decrease in the other coil. Sufficient gradient uniformity is obtained in a volume typically 5% of the coil dimension. The main disadvantage of this configuration is that, in order to obtain a reasonable movement range, large coils are required along with a corresponding large dissipation of power in vacuum. To alleviate this problem a relatively large permanent magnet dipole is used. A disadvantage of this scheme is that the absence of a magnetic field return yoke allows formation of large dimension open magnetic fields which can either perturb or be perturbed by external fields. Additionally, relatively large currents (and power dissipation) are necessary to produce the required forces.

We have designed a solution (Figure 1) that solves both problems and fully satisfies the requirements. The actuator we designed and implemented is made of a racetrack coil mounted on the IP table, floating in the confined magnetic field of a twin-gap magnetic yoke. The yoke is attached to the external reference structure and energized by two permanent magnets. A current passing through the coil will generate a force proportional to the integral of the yoke's magnetic field combined with the distributed current in the coil as in the vector equation 1. This arrangement does not generally produce a force that is independent of the relative position of the coil and the yoke. A careful design of both the coil and yoke solved this problem.

## **2. Conceptual design**

We started with the “voice coil” idea because the large magnetic yoke confines the magnetic fields, and allows large forces with small currents, power consumption, and exposure to perturbations. Normal voice coils have cylindrical symmetry and allow only unidirectional movement, while an IP allows free movement in the two horizontal directions.

A wire in a magnetic field will be subject to a force:

$$d\vec{F} = -i \vec{B} \times d\vec{l} \quad (1)$$

The Constant Force Actuator we devised replaces the voice coil cylindrical permanent magnet with two separated linear yoke gaps with opposite field directions. The coil is stretched in one direction to form a “racetrack”, and fits in the 2 yoke gaps as shown in Figure 1.

In our case B is parallel to the z direction and the coil wire runs in the x direction, on the flat surface where the force is exerted. The force F is therefore in the y direction. If the spires are evenly distributed on the coil, we can write the force exerted on the actuator coil as:

$$F_y = - \int_z \int_x B_z \sigma_x dx dz \quad (2)$$

Here  $B_z = B_z(x, y, z)$

$\sigma_x = \sigma_x(y)$  the current density in the plane xy which is in good approximation constant over the width and length of the coil.

#### 1) Optimization of $\partial F / \partial x = 0$

The coil is much longer than the magnet yoke and its wires are straight along axis x, straddling the yoke’s gap. Consequently any movement along axis x will not change the force defined in (2).

#### 2) Optimization of $\partial F / \partial z = 0$

The coils, which are much wider than the magnetic yoke gap and mounted at the center of the gap, integrate the same fraction of the vertical component of the magnetic flux for small variations in z. Additionally, the symmetry of the two gaps cancels out any force variation related to z movements. Therefore, the force F will not be modulated by vibrations in the z direction.

#### 3) Optimization of $\partial F / \partial y = 0$

In the y direction the coil enters and exits the yoke’s gap and can generate the largest variations of force. The voice coil force could be independent of the y position if the magnetic field were completely confined to the yoke’s gap volume. Unfortunately, this confinement is far from complete. The leakage magnetic field between the two arms of the yoke can be as much as 30% of the field in the gap itself (see Figure 2). The permanent magnet’s fringe field adds to this perturbation. As the coils move into the yoke,

it intercepts a growing fraction of this leakage field so that the total generated force will increase. This unwanted growth could be compensated by shaping the leakage field on both sides of the yoke.

In order to achieve  $\partial F/\partial y=0$ , we must compensate the leakage field around the coil so that the field gained on one side equals the field lost on the other side. This adjustment can be made by making B ‘quasi-periodic’ with respect to y, and choosing the width of the coil equal to the period of B(y).

We did this in four steps:

- 1) We added protrusions of the yoke beyond its gaps to generate a leakage field equal in shape and strength on both sides. The shape and length of the protrusion was chosen to optimize this effect.
- 2) We measured the vertical magnetic field intensity as a function of y, and obtained the graph of Figure 2.
- 3) We numerically integrated the measured magnetic field over the lengths of different coils and all possible positions to find the force applied to each coil.
- 4) To make the force constant, we adjusted the length of the coil and the shape of the yoke.

### 3. Actuator Construction and Optimization

Figure 2 shows the field of an optimized yoke. We observe that the magnetic field profile on the left of the peak is similar to that on the right. The field shape mimics locally a periodic function with a period of about 43 mm. By making a 43 mm wide coil, we can achieve constant force over a region of more than 10 mm in length. Figure 3 illustrates the steps used to optimize the coil width for the yoke of Figure 2. Of course, if the yoke is not well designed, no coil width will generate a constant force.

Table 1

Position y [mm]	0	20	40	60	80
Force [g]	193	193	192.5	192	192.5

#### **4. Prototype measurements**

After building the optimized coil and magnet's yoke, we placed the coil on a precision scale and suspended the magnet over it. We measured, at constant current, the change of the weight of the coil while moving the magnet along all three axis. Table 1 shows the measured magnetic force exerted on the coil for varying positions of the magnet along the Y axis. The standard deviation is only 0.4% over 80 mm.

Similarly, the force did not show any measurable change for movement in the Z direction.

Finally, Figure 4 shows the force measurement of the coil moving in the Y direction, in and out of the yoke's gap. The result agrees perfectly with the calculations of Figure 3. The standard deviation is less than 0.2% within the resolution of the measuring apparatus in the first 10mm, and 0.4% within the first 15mm.

Three additional points have been addressed in the actuator design:

1. Except for the actual coil wire, the coil was built without metal parts in the magnetic field. This was done to avoid induced eddy currents in a conductor generating uncontrolled damping forces<sup>[16]</sup>. The coil wire is very thin and uniformly wound, so that the magnetic field variation integrated over it is vanishingly small. The damping generated by the coil as a whole is null if the coil is driven by a high impedance current generator circuit.

2. The actuator is completely built with vacuum compatible materials, and can be baked at high temperature to satisfy ultra high vacuum requirements.

3. The actuator provides a force per unit current of 1 Newton/Ampere and with our coil driver, a peak force of 1 N (with a peak dissipation of 40 W). In normal working condition, the actuator only dissipates a few mW.

#### **5. Implementation in the SAS towers.**

The actuators described above have been installed on the SAS Inverted pendulum prototype, and successfully used in a Multiple-In-Multiple-Out configuration to damp the attenuation chain modes.

The large force capability of the instrument has come in handy to shake the SAS chain during the characterization of its attenuation performance. The force versus position stability was completely satisfactory, and did not produce any additional noise. At the time no attention was paid to the electronics noise.

The SAS system was commissioned in the 3meter Fabry Perot prototype for TAMA at the University of Hongo in Japan. During the commissioning, it was noted that the actuator was much stronger than necessary. As a consequence, the electrical noise of the coil driver, coupled with the large force per unit current of the actuator, injected too much electro-mechanical noise, which spoiled the performance of the IP as illustrated in Figure 5. In order to reduce the actuator's electrical noise below all other sources, its force per unit current was reduced by a factor more than one hundred. The actuator efficiency was reduced by a factor of 30 by replacing the original permanent magnets with much weaker ones. The remaining fraction of the required force per unit current reduction was obtained by reducing the driver electrical gain.

The replacement of the magnets changed the saturation level of the yoke, and this introduced an unacceptable 0.5%/mm force gradient, see figure 6, circles. This slope, coupled with the seismic noise at the actuator base, would have re-injected noise at the level of  $2.5 \cdot 10^{-10} \text{ m/Hz}^{-1/2}$  at 1 Hz (assuming 1 micron r.m.s. seismic noise and 5 mN standing force operation). This noise was ten times larger than the IP performance. The force versus position slope was nulled again by adding 7 mm shims on the outer horns of the actuator's yoke. The corrector shims reduced the force slope by more than one order of magnitude, as illustrated in Figure 6 by the measurements labeled with squares. This final change brought the seismic noise re-injection level below the IP noise floor.

Even with the reduced force per unit current, it is expected that the actuator will operate below 50 mW of dissipated power (10 mW necessary for full tidal corrections, the rest of the forces being picked up by tuneable parasitic springs).

The maximum force needed during operation is the force that is required during an earthquake to maintain the damping of the suspended chain.

Of course, chain damping can be maintained only as long as the ground does not shake the surrounding safety structures over distances larger than the mechanical end stops of the IP (10 to 12 mm in all directions). Below this excursion level, the maximum force required to maintain full damping is the static force required to move the IP to its end stops. The IP is designed for working below 30 mHz, which sets the maximum earthquake return force requirement between 30 and 50 mN. This force level can be achieved by the current drivers, even after the force per unit current degradation described above.

The Olympia, WA earthquake, that damaged the Hanford Gravitational Wave Interferometer, shook the ground by plus and minus 5 mm. This excursion would not have brought the IP to touch its end stops. Therefore, we expect that in an earthquake as large as Olympia's the SAS chains would not have been

affected, and maintained full damping. If the earthquake had been stronger, the actuator yoke itself would have acted as an unintended end stop, limiting the IP range to 7-8 mm in one direction. To avoid this, future yokes will be designed 50% wider to allow the full IP swing dynamic range. We understand of course that during earthquake damping, the actuator dissipates several Watts and warms up, but this heating will have no consequences because of the brevity of earthquakes.

## **6. Conclusions**

A low power, high linearity, non-contacting force actuator has been developed to control the advanced LIGO and TAMA IP motions, and to damp the SAS rigid body resonances. The force that the actuator generates is constant within 0.5% in the entire IP dynamic range, in all degrees of freedom, and thus does not re-introduce seismic noise above the level of all other residual noise sources. The actuator current-to-force ratio was initially so high that it had to be reduced to keep its electronics noise contribution below the other sources of noise. Even with the reduced ratio, the actuator and its driver are capable of providing the forces necessary to maintain full chain damping during sizeable earthquakes.

## **7. Acknowledgments**

This research is supported by the National Science Foundation under Cooperative Agreement PHY98-01158.

We are indebted to the Virgo electronics group that provided us with the coil drivers circuit design.

We also wish to thank Professor Eugene Cowan for his insightful comments and suggestions.

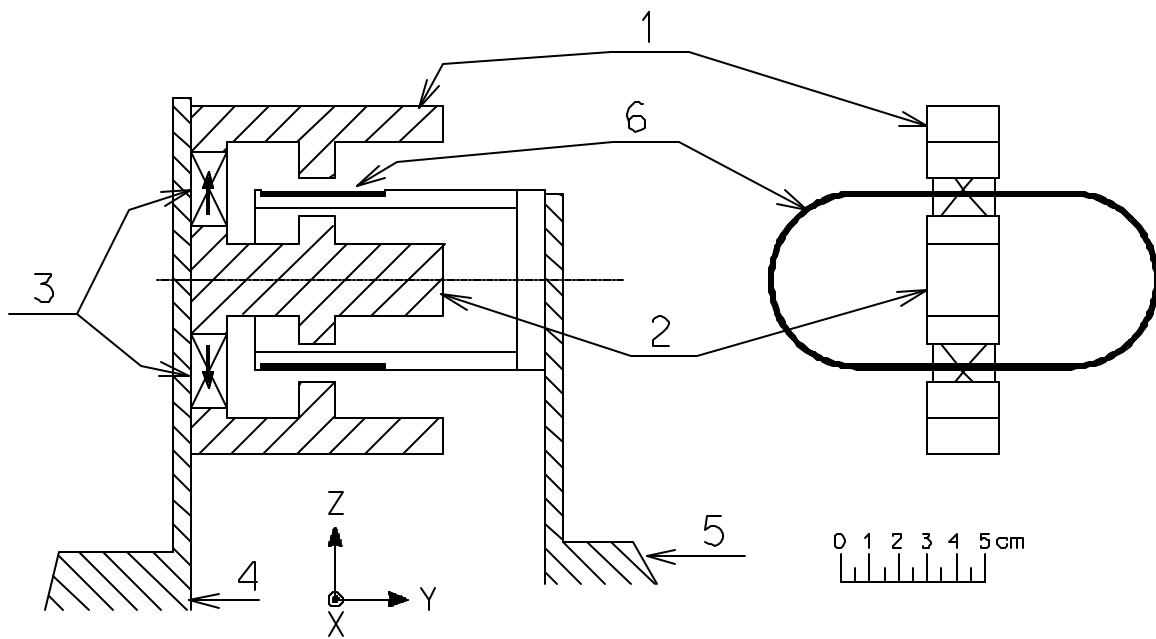


Figure 1:

Schematic view of the non contacting actuator. Side view (left side) and front view (right side).

- 1. Yoke jaws, 2. Yoke central bar, 3. Permanent magnets (the arrows in the magnet indicate the field direction),
- 4. Mechanical support on the fixed structure, 5. Mechanical support on the Inverted Pendulum, 6. Racetrack coil.

For simplicity the mechanical supports are only sketched on the side view. The Cartesian axis refers to the side view.

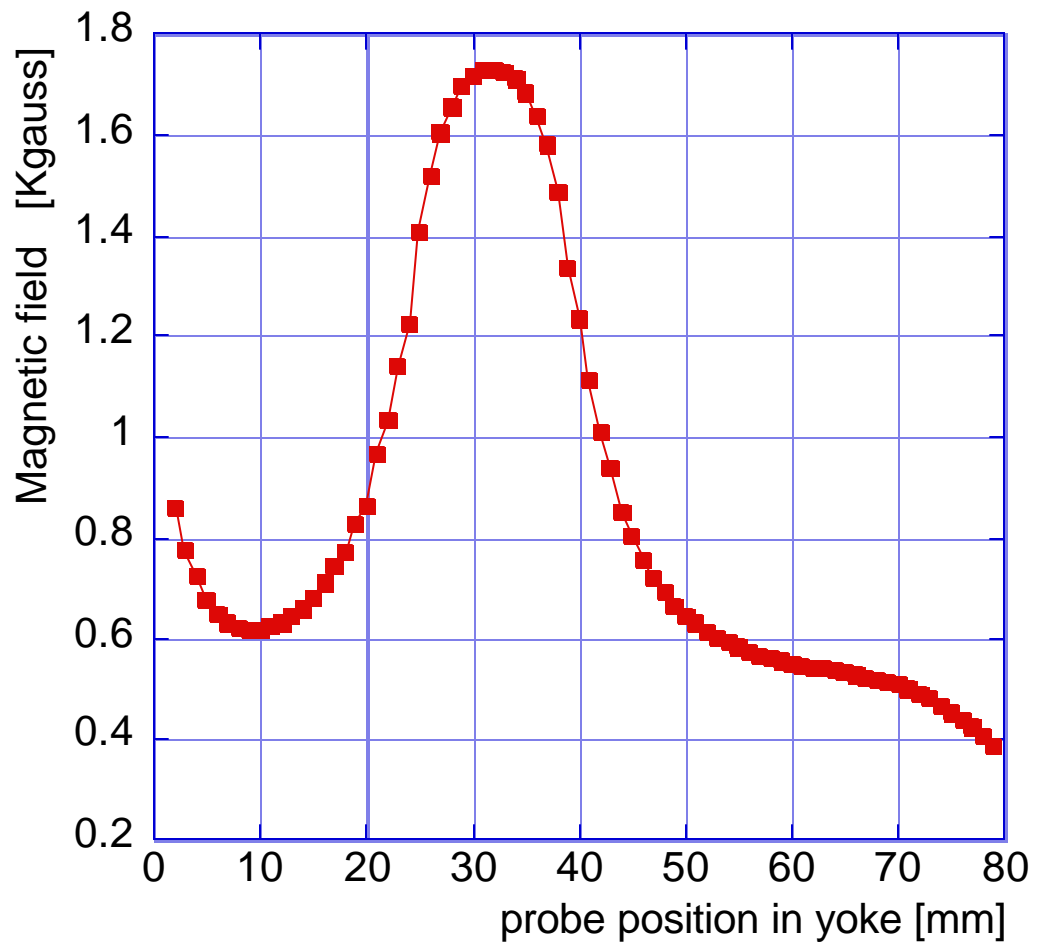


Figure 2: Magnetic field profile as a function of the y position.

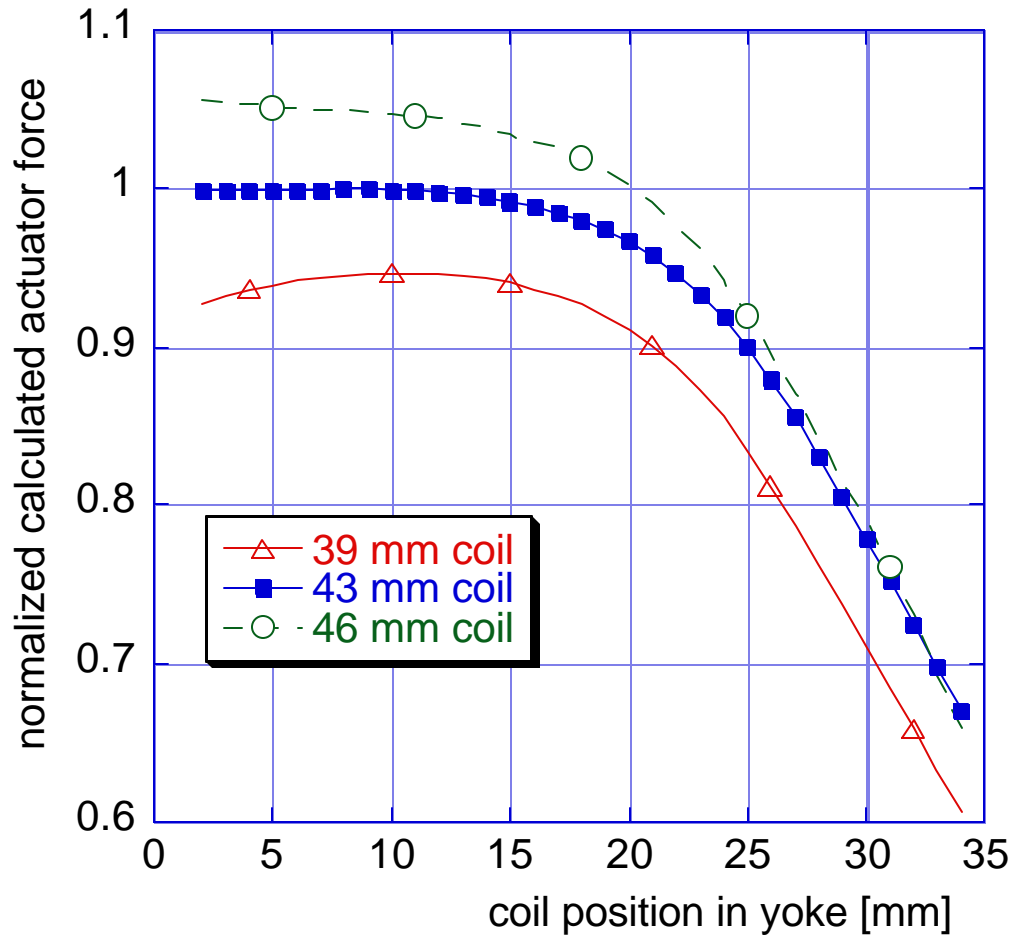


Figure 3: Calculated Y force amplitude for coils of different widths moving inside the yoke field of figure 2.

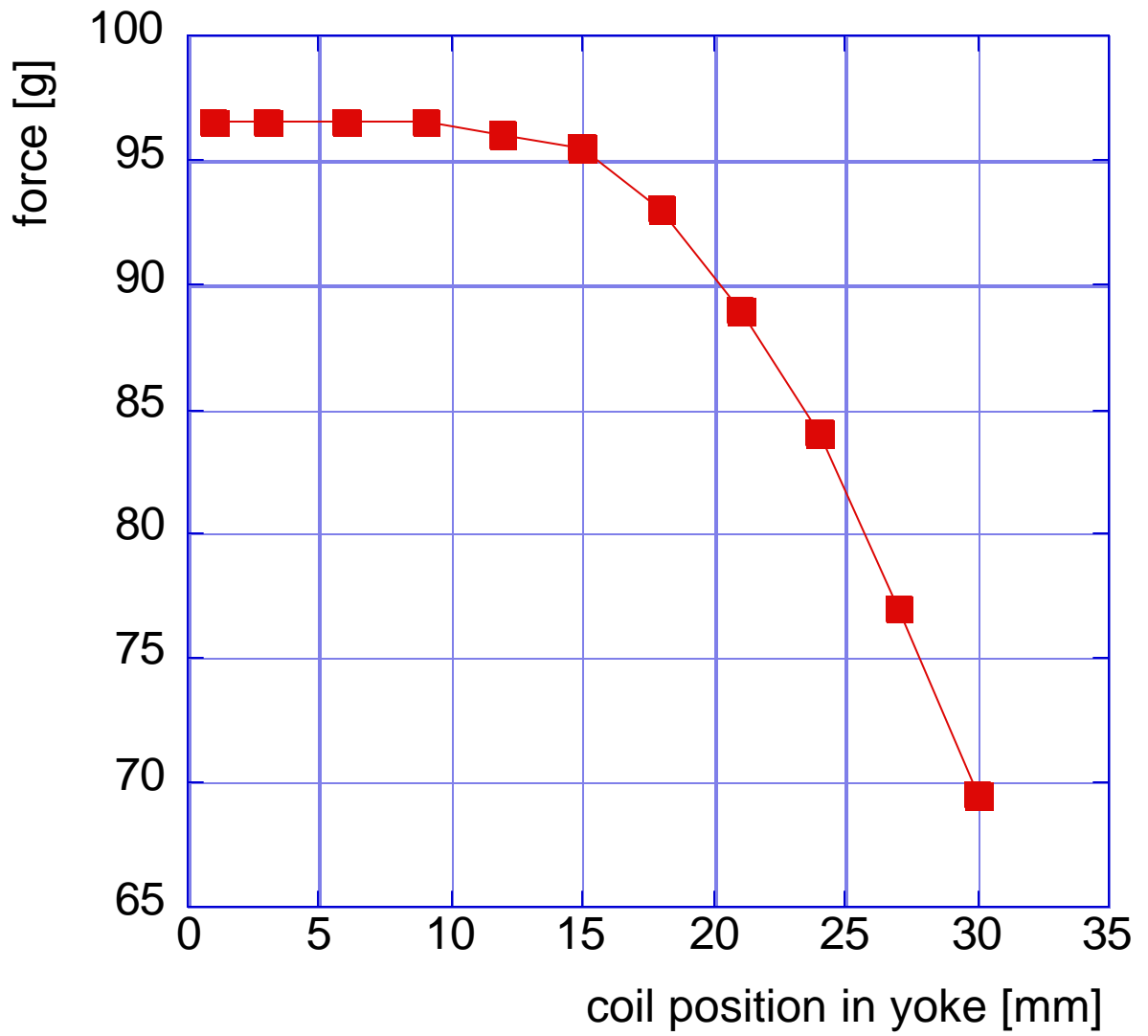


Figure 4: Force measured on a scale as the coil is moved micrometrically outside the yoke's gap.

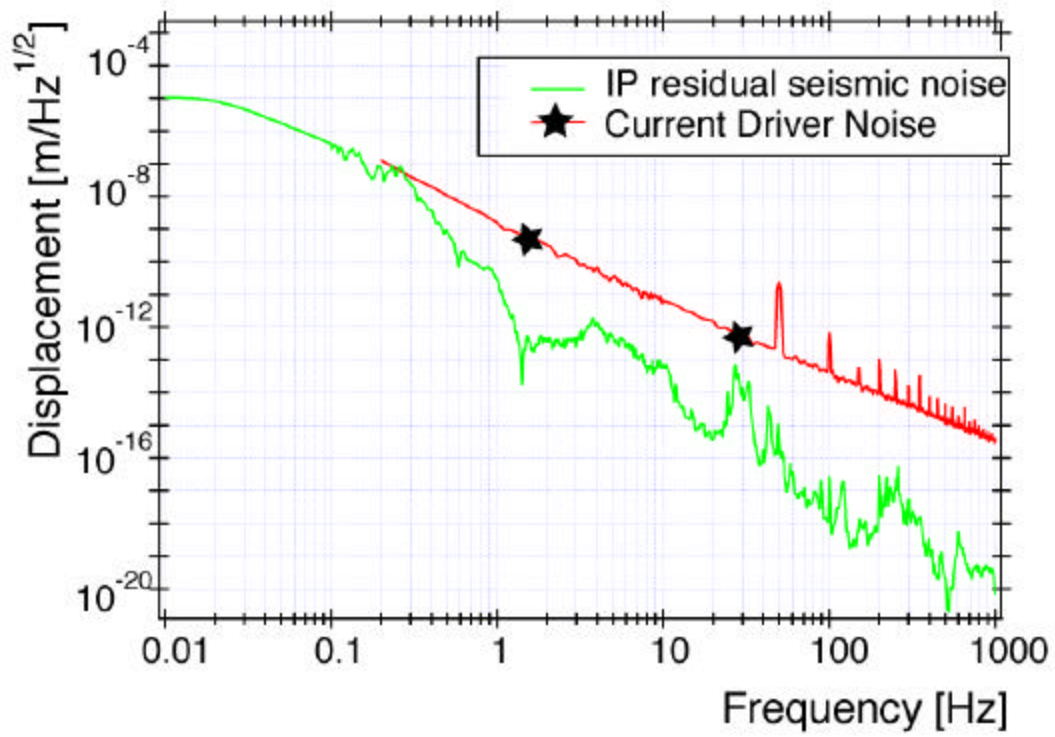


Figure 5: Comparison of the residual seismic noise on the passive IP platform and of the driver's electrical noise feeding into the actuator. The actuator gain would be low pass filtered below 3 to 5 Hz but it would still dominate over the IP mechanical noise. The actuator force per unit current has to be reduced by at least a factor of 100.

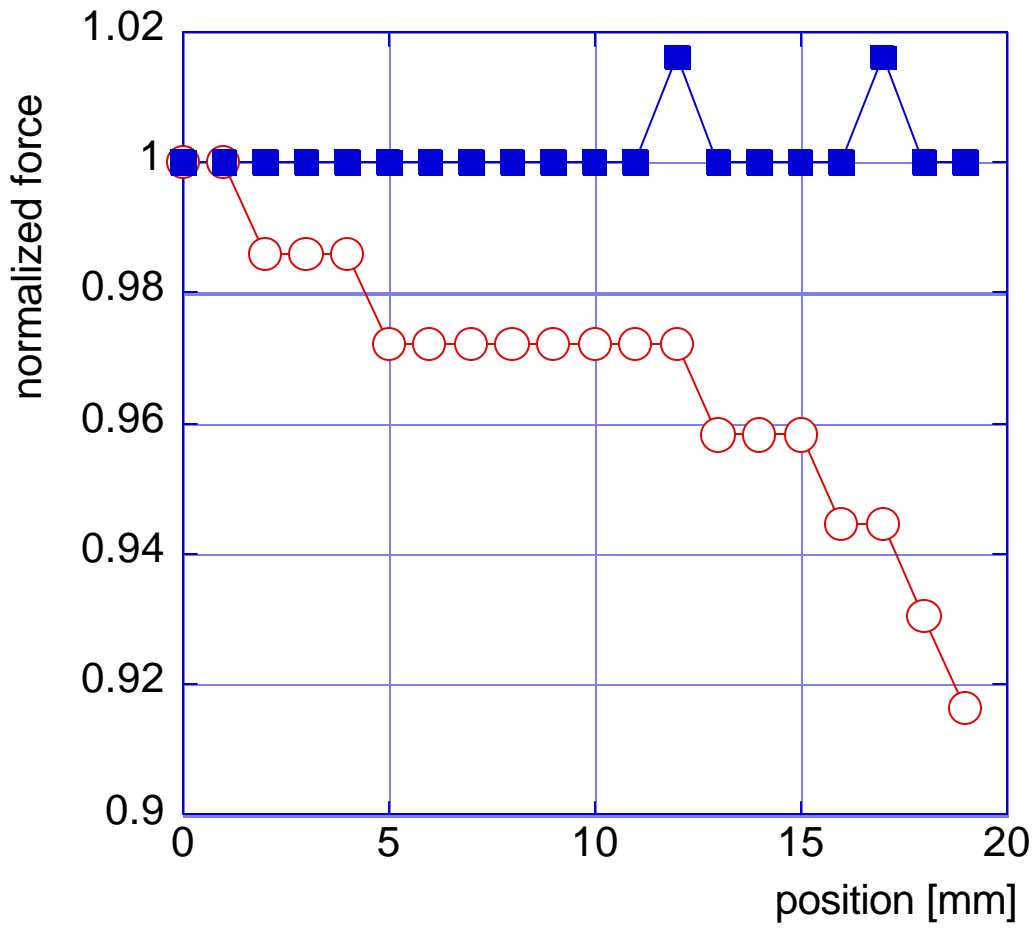


Figure 6: Actuator force versus y position after replacing the magnets (circles) and after re-shimming the yoke. The 0.5%/mm slope was eliminated by the shims (squares). The quantized jumps in the plot correspond to the scale digitalization noise (10 mg). The force drops rapidly (2%/mm) above 20 mm.

## 8. References

- 
- [<sup>1</sup>] Alessandro Bertolini, et al., “New Seismic Attenuation System (SAS) for the Advanced LIGO Configurations (LIGO2)”, proceedings of 1999 Amaldi conference, Pasadena, CA.
- [<sup>2</sup>] G. Losurdo et al., Inertial controls of the mirror suspensions of the Virgo interferometer for gravitational wave detection” **Rev. Sci. Instrum.**, Vol 72, no 9, p. 3653, 3661, (2001)
- [<sup>3</sup>] G. Losurdo, “Inertial control of the Virgo superattenuators”, proceedings of 1999 Amaldi conference, Pasadena, CA.
- [<sup>4</sup>] G. Ballardini, et al., “Measurement of the Virgo superattenuator performance for seismic noise suppression”, **Rev. Sci. Instrum.**, Vol 72, no 9, p. 3643, 3652, (2001)
- [<sup>5</sup>] J. Winterflood, et al. AIP conference proc. (1999)
- [<sup>6</sup>] G.Losurdo, et al.: “An inverted pendulum pre-isolator stage for VIRGO suspension system”, **Rev. Sci. Instrum.**, **70**, 2507-2515 (1999)
- [<sup>7</sup>] M.Beccaria, et al. “Extending the VIRGO gravitational wave detection band down to a few Hz: metal blade springs and magnetic antisprings”, **Nucl.Instr.and Meth. in Phys.Res. A**, 394, 397-408, 1997.
- [<sup>8</sup>] R.De Salvo, et al. “Performances of an ultralow frequency vertical pre-isolator for the VIRGO seismic attenuation chains”, **Nucl.Instr.and Meth. in Phys.Res. A**, **420**, 316-335 (1999)
- [<sup>9</sup>] A. Bertolini et al. “Recent progress of the R&D program of the Seismic Attenuation System (SAS) proposed for the Advanced Gravitational Wave Detector, LIGO II”, proceedings of “8th Pisa Meeting on Advanced Detectors (May 21-27 2000, Isola d'Elba, Italy)”
- [<sup>10</sup>] G. Cella, et al., “Seismic Attenuation Performance of the first prototype of a Geometrical Anti Spring Filter”, submitted for publication to **Nucl.Instr.and Meth. in Phys.Res.**, 2001
- [<sup>11</sup>] J. Winterflood, et al., Phys. Lett. **A 263**,9 (1999)
- [<sup>12</sup>] J. Winterflood, et al., , Phys. Lett. **A 243**,1 (1998)
- [<sup>13</sup>] G. Ballardini, et al., “Measurement of the transfer function of the steering filter of the Virgo super attenuation suspensions”, **Rev. Sci. Instrum.**, Vol 72, no 9, p. 3635, 3642, (2001)
- [<sup>14</sup>] H.Tariq, et al., “The Linear Variable Differential Transformer (LVDT) position sensor for Gravitational Wave Interferometer low-frequency controls”, in preparation

---

<sup>[15]</sup> Alessandro Bertolini, “High sensitivity accelerometers for gravity experiments”, Doctoral thesis, Universita’ di Pisa, June 2001, available at [www.LIGO.caltech.edu](http://www.LIGO.caltech.edu)

<sup>[16]</sup> Akiteru Takamori, et al., “Mirror Suspension System for the TAMA SAS” to appear in the proceedings of the 4<sup>th</sup> Edoardo Amaldi Conference on Gravitational Waves, Perth, Australia, 8-13 July, 2001. Preprint ref. LIGO-P01033-00-D available at <http://admdbsrv.ligo.caltech.edu/dcc/>

<sup>[17]</sup> Lee Hollonay, Private Communication.